# Dynamic Plasticity in Solid Solution: Observations and Quantification

R. Shabadi, H. J. Roven, E. S. Dwarakadasa, S. Kumar

*Measurements were performed on three different alloys, AA 5082, AA 7020 and AA 2219 for the behaviour of strain bands associated with the Portevin Le-Chatelier effect occurring at room temperature upon tensile testing. A newly developed laser speckle technique (LST) was used in-situ during testing. The technique facilitates a clear knowledge about the strain band characteristics, in particular, the band velocity Vband, and the bandwidth Wband.*
*The knowledge obtained with the LST was useful for understanding the underlying mechanisms for the formability limit when negative strain rate sensitivity is active.*

Parole chiave: alluminio e leghe, prove meccaniche

## INTRODUCTION

Aluminium alloys are increasingly used as a construction material due to their light weight, environmental friendliness, excellent corrosion resistance and easy shape change capability after or during semi-product manufacturing, e.g. extrusion. The alloys can be designed for optimised forming properties and final product properties such as strength, fatigue resistance, crash worthiness, surface quality, etc. However, the traditional alloys have only a moderate resistance of strength properties against temperature. This in fact improves the workability and thereby the low-cost criteria demanded in the market. In cold forming operations such as profile forming and deep drawing, intrinsically governed phenomena such as the negative strain rate sensitivity of the material is known to reduce the formability.

A more recent review [1] has considered a range of microstructural and mechanical influences on dynamic strain aging (DSA) and hence the rate sensitivity. One of the most regularly observed macroscopic manifestations of DSA is a discontinuous record of the plastic deformation, commonly referred to as serrated flow or the PLC effect. Dynamic Strain Aging and therefore manifestations of DSA, including serrated flow are evident within a specific regime of deformation parameter such as strain, strain rate, temperature and strength. In the case of aluminium alloys, this regime frequently includes deformation at ambient temperatures and at strain rates within a range, which is typical of industrial forming operations such as profile and sheet metal forming.

Efficient DSA requires rapid interaction between solute atoms and mobile dislocations. In BCC metals, this rapid interaction matches the asymmetric stress fields of a single interstitial with the neighbouring dislocation stress field and hence continuously increases dislocation glide resistance. In FCC metals the stress fields around single solute atoms are volumetrically symmetric. Hence, no strong interaction exists between single solute atoms and dislocations. A pair of substitutional and interstitial atoms located in neighbouring lattice sites create an asymmetric stress field, which can rapidly change its orientation by moving the interstitial atom from one interstice to another, around the substitute. This enables rapid matching of solute pair stress fields with the dislocation stress field. It is known that DSA improves strength properties at elevated temperatures and enhances fatigue strength in metals with BCC crystal structure. It has been shown [2] that by proper alloying it is possible to introduce DSA and enhance fatigue strength also in FCC materials. For certain deformation conditions, such as tension (Wijler [3]), compression (Kocks [4]) and torsion (McCormick [5]), negative strain rate sensitivity of the flow stress may result in discontinuous yielding observed as repetitive stress serrations in the stress strain curve. The corresponding deformation behaviour is normally associated with propagative strain carriers, such as Lüders type or Portevin Le-Chatelier type of instabilities. In the present work only the PLC type of bands are considered due to their dominant role in plastic behaviour of several aluminium alloys.

Formability of sheets and profiles can be assessed by the material parameters; r (plastic strain ratio), n (work hardening coefficient), $e_u$ (uniform strain) and m (strain rate sensitivity) determined from the uniaxial tensile tests. In stretching the ability of a metal to resist strain localisation and hence local thinning, is the most important material property. The uniform strain represents in this regard a most critical factor to describe stretching ability - especially when the material under consideration has a negative strain rate sensitivity [6]. The propagating bands typical of DSA are characterised by their velocity, width and associated strain. In the present work, some of these characteristics are determined experimentally by an in-situ Laser Speckle Technique (LST). The influence of grain morphology and alloy chemistry was studied applying three different aluminium alloys in their solid solution condition. The goal was to understand the relationship between DSA and the formability limit physically manifested as shear band formation.

**Rajashekhar Shabadi, E.S. Dwarakadasa, Subodh Kumar**
*UGC Centre for Advanced Studies, Department of Metallurgy, Indian Institute of Science, Bangalore, India*

**Hans Jørgen Roven**
*The Norwegian University of Science and Technology, Department of Materials Technology and Electrochemistry, Trondheim, Norway*

Paper presented at the 7th European Conference EUROMAT 2001, Rimini 10-14 June 2001, organised by AIM

## EXPERIMENTAL PROCEDURE

### Materials

The materials used were of commercial interest aluminium alloys, labelled alloy AA 7020, AA 5082 and AA 2219. The alloys were received as 1mm rolled sheets except for the 5082 that had a 2.3 mm thickness. The actual alloy compositions are shown in Table 1.

Before uniaxial tensile straining all specimens of alloy 7020

| Alloy | Weight percent of alloying elements Zn | Mg | Cu | Zr | Al |
|---|---|---|---|---|---|
| AA 5082 | 0.021 | 3.00 | 0.07 | - | Balance |
| AA 7020 | 4.05 | 1.18 | 0.044 | 0.11 | Balance |
| AA 2219 | 0.012 | 0.011 | 1.52 | 0.116 | Balance |

*Table 1. Actual chemical composition of the investigated alloys in wt%*

*Tab. 1. Composizione elementare, % peso, delle leghe studiate*

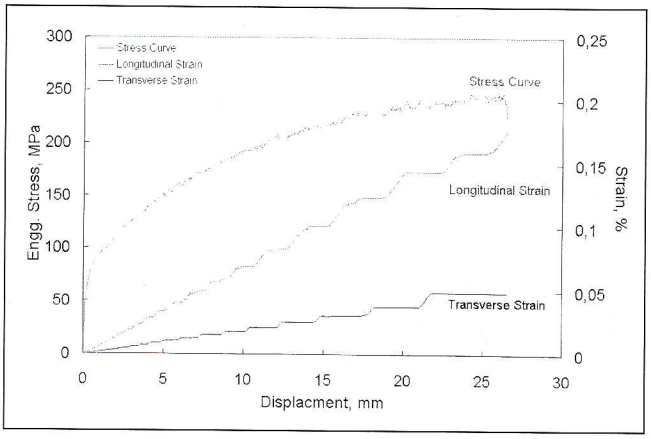


*Fig. 1. Typical stress-displacement curve and corresponding extensometer strain evolutions obtained from the deformation experiments with in-situ LST. Initial strain rate was $1x10^{-3}s^{-1}$ and the alloy was AA 7020.*

*Fig. 1. Tipica curva sollecitazione-spostamento e corrispondenti evoluzioni di deformazione rilevate dall'estensimetro ottenute mediante gli esperimenti di deformazione con LST in situ, per una velocità di deformazione iniziale di $1x10^{-3}s^{-1}$ e per la lega AA7020.*

were solution heat treated (W-temper), i.e. 480 0C for 30 minutes followed by quenching in water (20 0C). Correspondingly, for the 5082 alloy, the solution treatment was 550o C for 1hr, and the 2219 alloy was tested in the as-received (annealed condition). Testing of W-tempered alloys was done within 10 minutes after finishing the solution treatment.

## Deformation experiments

Uniaxial tensile experiments were carried out in a universal-testing machine of the type MTS 880. All experiments were performed with a constant displacement velocity. Specimens were machined in the rolling direction ($\alpha = 00$), and dimensions were 2.3mm or 1mm thickness, 60mm parallel length and width 12.7mm.

Different initial strain rates from $1x10^{-4}s^{-1}$ to $1x10^{-1}s^{-1}$ were applied, with two different extensometers mounted in separate positions along the specimen gauge length. One measured the transverse and the other the longitudinal strain.

Fig.1. shows the typical engineering stress-displacement curve obtained from the double extensometer method. If the PLC bands are travelling outside an extensometer gauge length, no strain increment will be registered by this extensometer. However, if the band is present within the other extensometer gage, this will register a strain increment in the same time interval of the test. The experimental stress data is, due to the discontinuous nature of the extensometer strain in the present case plotted against the stroke displacement. The serrated stress, in this case, can easily be imagined in the shown plot.

From the above observations it can be stated that when more strain is added to the specimen gage length, the increment is concentrated in the PLC band, which travels along the gage length in the applied stress direction. Hence, the PLC bands can be referred to as propagative strain bands, e.g. the plasticity actually taking place is dynamic.

## The Laser Speckle Technique (LST)

All alloys revealed a typical PLC type of plastic flow when subjected to uniaxial tensile stresses at room temperature. It was of interest to "record" the PLC bands or zones as they were moving along the specimen gauge length during plastic straining. It was achieved by arranging a special device set-up, called the Laser Speckle Analyser. Here, a laser beam is used as the source of radiation and it was expanded in order to cover the whole gauge length surface. The speckle pattern obtained from the beam reflected from the as machined surface was observed through an ordinary video camera. This camera has a capacity of grabbing 25 pictures per second. The camera is connected to the image grabber and then to a computer, which uses specially developed software together with SnabGrab 1.0 to grab and further analyse the images, which were taken from the camera. The stored images are analysed by subtracting images one from the other. With this system there are basically two different ways of creating subtracted images:

1. Raw images can be subtracted in accordance with the following:

   $n = n - (n - 1)$ (1)

   where 'n' is the chronological number of the image, which is subtracted from the previous image (n-1). This method is used in the present study.

2. Raw images can also be subtracted in the following way:

   $n = (n - k)$ (2)

   where 'k' is any integer 1, 2, 3 .. etc. (This method was not applied in the present case.)

The idea is based on the theory of change in speckles appearing on the sample surface. A rough surface illuminated by an expanded laser beam looks grainy due to the coherence properties of the laser light. This grainy appearance is called a speckle pattern. A band, propagating through the material

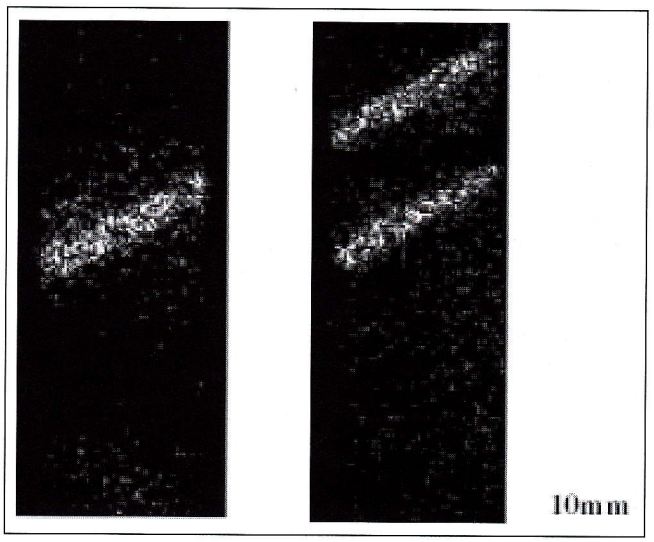


*Fig. 2. Images of PLC bands after raw images have been processed by the subsequent subsequent subtracting method of LST. Initial strain rate was $1x10^{-3}s^{-1}$ and the alloy was AA 7020.*

*Fig. 2. Immagini di bande PLC dopo elaborazione delle immagini grezze mediante il metodo di sottrazione successiva del LST. La velocità di deformazione iniziale era $1x10^{-3}s^{-1}$ applicata alla lega AA 7020.*

*Fig. 3. Grain morphologies of the alloys investigated as viewed in the long transverse plane a) AA 5082, b) AA 7020 and c) AA 2219.*

*Fig. 3. Morfologie del grano delle leghe, rilevabili nel piano trasversale lungo, relative alle leghe: a) AA 5082, b) AA 7020 e c) AA 2219.*

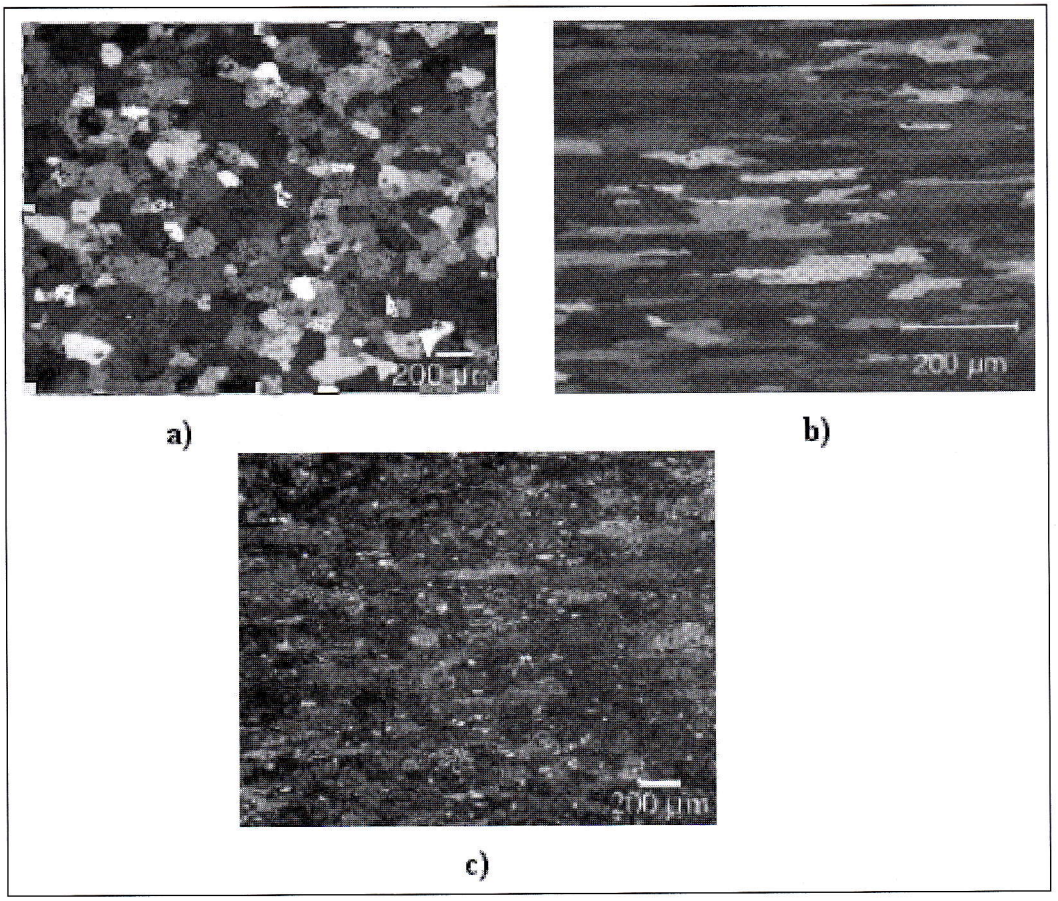


volume, causes a disturbance in the speckle property of the material illuminated from a diffused laser beam. This is due to the fact that all deformation seems to be localised within such a band or zone while straining. When zones are moving due to the applied stroke displacement, the region between the just deformed and the one that is going to be deformed, i.e. the front of the propagating PLC zone, will exhibit different reflection properties as compared to the surrounding specimen areas, e.g., see also ref. [7].
Further details of this technique are as follows:

- All components were aligned in such a way that the maximum intensity of the reflected speckle is grabbed into the camera. This can be achieved from keeping the laser gun and video camera unit in vertical alignment.
- As soon as the straining of the specimen is started, time the image grabbing is activated in the computer. All the true time images were stored in a sub-directory in the name specified by the user. After saving the images, the results were analysed in accordance with the above mentioned method.
- By just comparing two near subsequent images nothing will be observed. However, when as intensity subtraction is performed, even very small changes in the intensity can be observed. In the case of a moving PLC zone, this difference in intensity is on a length scale equal to the zone width and it will appear as a bright area, i.e. see Figure 2.

## RESULTS

### Microstructural Studies

The grain morphologies of the three different alloys are shown in Figure 3. The AA 5082 alloy has recrystallized grains. The as received alloy was in the rolled condition. The alloy has been given a solutionising treatment so as to simulate the practical forming practice of the material during industrial processing. The grain size of the alloy has been measured from the linear intercept method and found to be of the order of 60 µm.
In contrast to the alloy 5082, the microstructures of AA 7020 alloy has no recrystallisation and the grain size is approximately 80-90 µm and ~400 µm in the thickness and length direction respectively. The material was in T6 condition as received. As industrial practice to form the parts into different shapes, the material was given a solution treatment of 480 °C for 1 hour. A comparison of the two microstructures before and after the solution heat treatment did not reveal any change in the grain size or morphology. The alloy AA 7020 had irregular shaped inclusions in the normal direction and at the surface as observed from the long transverse direction, these inclusions of irregular shapes are assumed to be a result of the precipitation of either $\alpha$-$Al_{12}FeSi$ or c-Al (Fe, Mn) Si.
Microscopical examination of the alloy AA 2219 revealed that the grains were heavily banded in the direction of working. From the Fig.3(c), the alloy AA 2219 with high contrast spots it is evident that there have been certain inclusions along the grain boundaries and some in the grain interior. The degree of banding was more severe in comparison with the other alloys studied, and the elongated grains were larger near the surface. The brighter spots observed in the micrographs are due to the precipitated $CuAl_2$ particles and insoluble particles, probably of the $Mn_3SiAl_6$ composition.

### LST Results

Figure 4 shows the band velocities recorded from the laser speckle technique for all alloys studied at the initial strain rate of $1x10^{-3}$ $s^{-1}$. The 5082 alloy had the higher velocity when compared to that of the AA 7020. For the alloy 5082, the initial velocity was around 50mm/s and it was constantly decreasing to until it reached the UTS where the velocity was ~14mm/s. However, the alloys 5082 and 7020 did not

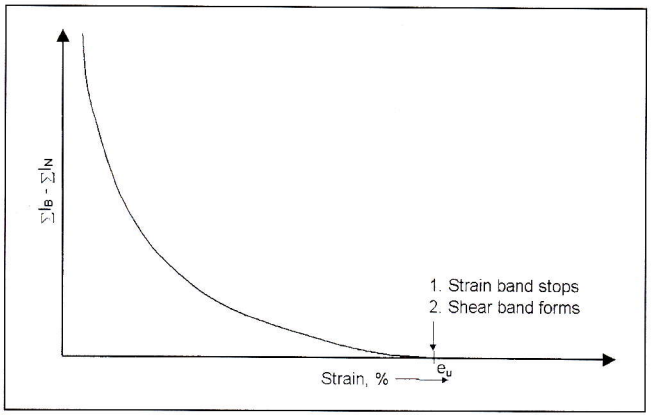


*Fig. 6. Schematic drawing of the mechanism behind onset of plastic instability (shear banding) in materials with active DSA.*

*Fig. 6. Disegno schematico del meccanismo alla base dell'inizio dell'instabilità plastica (shear banding) in materiali con DSA attiva.*

containing copper as the main alloying element. The reason for this is probably due to the relatively large atomic size mismatch of Cu as compared to the Al atoms (-10.5% difference), hence, giving strong dislocation-solute interactions and the need to 'escape' for the band prevails. The strain bands observed with the AA 2219 could therefore be attributed to the DSA phenomenon occurring in the material, although, the magnitude of serrations was very less.
The 2219 alloy did also exhibit a clear characteristic of a band velocity reaching a plateau after certain amount of straining.
This indicates that the atomic mismatch plays a more important role than the diffusion rate as far as PLC behaviour is concerned.
From Figure 5, it can be noted that the higher amount of magnesium present in the AA 5082 alloy also calls for a wider band. The increasing width with plastic strain can be attributed to the enhanced work hardening rate with high magnesium or copper contents. In contrast, the low magnesium content in AA 7020 is less than with AA 5082 and offers lesser dislocation pinning thereby reducing the bandwidth. The increasing band width observed in all the alloys can be attributed to the forest of dislocations that is left behind during each pass of the strain band. All the alloys exhibited maximum bandwidth at the uniform strain. At this point the sum of interactions between solutes and dislocations in the band ($\Sigma I_B$) and the sum just infront of or behind the band ($\Sigma I_N$) are approaching equality. So, there is no plasticity gained by an additional movement of the band. Hence the band movement seizes and the dormant plastic instability sets in. This situation can be illustrated as shown in the Figure 6.
After the instability point, the shear band carries all incremental plastic strain and at the same time it deforms in pure plane strain mode i.e. the thickness reduces. Hence, the nominal stress falls and plastic strain is even more localised. Just before the fracture the shearing activity is very localised – probably of the order of a few atomic distances. And, the local plastic strain rate is accordingly high.
By this, the present LST is believed to give valuable qualitative and quantitative information on physical mechanism governing formability at room temperature in negative strain rate sensitive materials.
In the above discussions one have made conclusive comments which rely on mechanisms connected to solute-dislocation interactions and the differences in their interactions among the different alloying elements (Mg, Cu and Zn). As observed from Figure 2, the grain morphologies are quite different. From the morphologis of AA 2219 and AA 7020, one should expect higher band velocities due to shorter free dislocation glide distances in comparison to the alloy AA 5082. But the experimental observation of the band velocity vs strain increment (Figure 4) shows the opposite trend. This means that the overall controlling mechanism for band parameters and the onset of plastic instability is primarily atomistic. Hence, grain morphology seems to have less influence on band characteristics.

## CONCLUSIONS

From the present investigations the following conclusions can be drawn:

1. All alloys investigated in the solution heat treated condition demonstrated a clear DSA-PLC phenomenon at strain rates $1x10^{-3}$ - $1x10^{-4}$ $s^{-1}$, but was also observable at $1x10^{-1}$.
2. The band characteristics are controlled by atomistic interaction and not by grain morphology, i.e. the DSA phenomenon.
3. The "formability limit" is reached when the PLC band rate reaches its lowest rate regime and onsets the shear band formation.
4. The in-situ experience obtained through a laser speckle technique is very useful in order to understand and characterize the propagative nature of the PLC phenomenon and the formability limit of the material.

## ACKNOWLEDGEMENTS

Authors are indebted to Indo-Norwegian collaboration programme ALTECH and Hydro Aluminium AS for the financial support extended to carry out the above research. Authors would also like to thank Mr.Vikhagen, Optonor AS Norway for the help in developing the laser speckle technique and the software for the same. The previous work of Dr. A. Søreng (now Raufoss ASA) is also appreciated. Authors are thankful to M/s Hindustan Aeronautics Limited and Raufoss ASA for supplying the material for the above study.

## REFERENCES

1. J. M. ROBINSON, International Materials Reviews, 39, No.6 (1994), p217-227.
2. T.TIANEN, V.T. KUOKKALA, J. VUORINEN, et. al , The 3rd International Conference on Aluminium Alloys, p191-196.
3. WIJLER, A., SCHADE VAN WESTRUM, J and VAN den BEUKEL, A., Acta. Metall. 20, (1972), p. 355
4. MULFORD, R.A. AND KOCKS, U.F., Acta. Metall., 27, (1979), p.1125.
5. McCORMICK, P.G., Acta. Metall., 30, (1982), p. 2079.
6. H.J. KLEEMOLA and J.O. KUMPULAINEN, Sheet Metal Industries, (1978), p. 703-713
7. A.SORENG and H.J. ROVEN, Proc. of Advanced Light Alloys and Composites, 5-15 September, 1997, Zalcopane, Poland.
8. ERIC A BRANDES, Smithells Metals Reference Book, 6th Ed. Butterworth & Co (Publishers) ltd., (1983).
9. B.J. BRINDLEY and J.B WORTHINGTON, Metallic Rev. 15,(1970), p. 101.

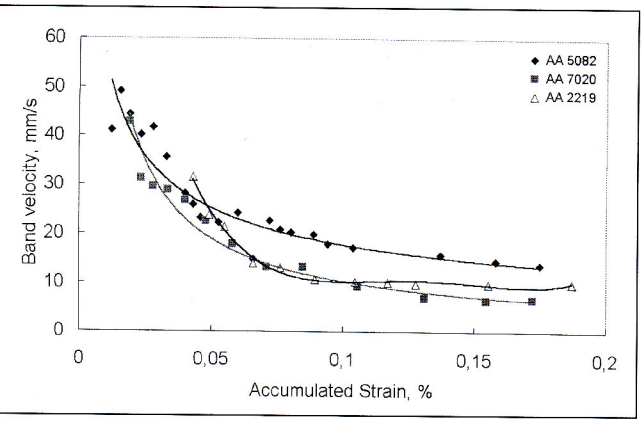


*Fig. 4. Band velocity versus accumulated strain curve, for different alloys tested at $10^{-3}$ $s^{-1}$ at room temperature.*

*Fig. 4. Velocità di banda in rapporto alla curva della deformazione accumulata, per le diverse leghe sollecitate a temperatura ambiente e a $1x10^{-3}s^{-1}$.*

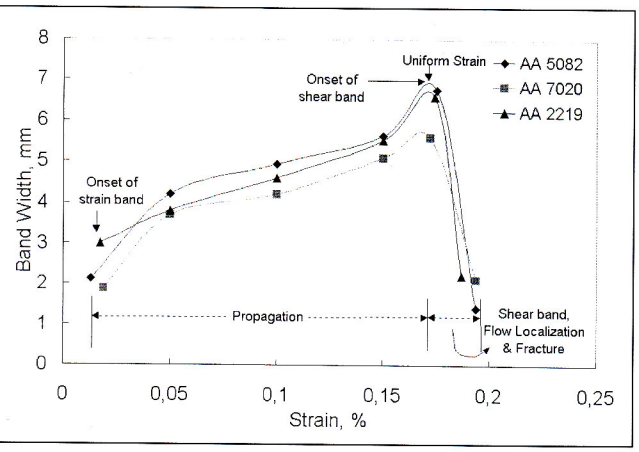


*Fig. 5. Band width versus displacement curve, for different alloys tested at $10^{-3}$ $s^{-1}$ and at room temperature.*

*Fig. 5. Larghezza della banda in rapporto alla curva di spostamento per le diverse delle leghe analizzate a $1x10^{-3}s^{-1}$ a temperatura ambiente.*

| Metal (B) | Solute (A) | DAB ($Cm^2$ $s^{-1}$) |
|---|---|---|
| Aluminium (20 °C) | Zn | 0.246 |
| | Mg | 0.061 |
| | Cu | 0.611 |

*Table 2. Approximate diffusivities of actual alloying elements in aluminium, (after Smithels [8]). Diffusivity data shown in Table 2 is calculated from extrapolating the data quoted in Smithels [8])*

*Tab. 2 – Diffusività approssimativa degli elementi alliganti nell'alluminio (dopo Smithels [8]).*

| Atoms of | Atomic radius, r (Å) | % mismatch = [(rx-rAl)/rAl] X 100 |
|---|---|---|
| Al | 1.43 | - |
| Mg | 1.60 | + 11.9 |
| Zn | 1.33 | - 7.0 |
| Cu | 1.28 | - 10.5 |

*Table 3. Atomic mismatch of aluminium atom with different alloying elements.*

*Tab. 3 - Sbilancio atomico dell'atomo di alluminio con diversi elementi alliganti.*

show the constancy in velocity at large deformations, as was the case with alloy 2219. AA 7020 had the initial velocity of ~42mm/s and reached the speed of a ~6mm/s at ultimate tensile strength. Similarly, alloy 2219 exhibited the velocity of ~30mm/s and reached a plateau at ~10mm/s. The latter alloy also exhibited the character of strain band reaching a plateau after certain amount of deformation.

The band widths recorded for different alloys during the laser speckle recording are shown in Figure 5. The curves can be divided into four different regions: onset of strain band, propagation, shear band formation and final fracture. All the alloys exhibited the nature of increasing band width with strain accumulation in the specimen. From the onset of band formation up to ~5% deformation the band width increased rapidly. Beyond ~5%, the band width still increased although at a lower rate. As observed from the in-situ LST, the strain bands seem to halt at the uniform strain, thereby, forming flow localisation leading to a shear band which later fractured. It is evident from the Figure 5 that AA 5082 has the largest band width in comparison with the other two alloys. It can be noted from the same figure that the shear band widths are more narrow than the PLC band present just before the transition.

## DISCUSSION OF THE EXPERIMENTAL RESULTS

The propagating deformation bands, usually referred to as PLC bands were caught in-situ with the help of the Laser Speckle Technique. All alloys showed the pronounced PLC effect in the tested conditions, and at applied strain rates. The PLC effect was more pronounced at the lower strain rates like, $10^{-4}$ and $10^{-3}$ $s^{-1}$ but was also observable at $10^{-1}$ $s^{-1}$. For the present discussions one will take only the case with $10^{-3}$ $s^{-1}$, because this strain rate promotes a very typical PLC behaviour in all alloys tested. As known, the PLC effect is a manifestation of dynamic strain aging and the present studies could support that the DSA is the main cause of the PLC effect. The following discussion will concentrate on the parameters obtained from the LST.

It is quite evident that the presence of magnesium and zinc in solid solution caused the PLC effect in AA 5082 and AA 7020 alloys and copper in the AA 2219 alloy. The band velocity exhibited a character of reaching a more or less constant velocity after a certain amount of straining (see Figure 4). The band velocity was higher with the AA 5082 alloy corresponding to the AA 7020 and the serrations were of B-type [9]. As AA 5082 contains 3.00wt % Mg, this alloy obviously has the maximum reach to the dislocations for pinning them down, at the same time the dislocation density which tries to escape through the obstacles is also high (e.g. a high work hardening rate). Because of a higher diffusion frequency with higher Mg content, the strain bands need to have higher speeds to carry the strain through the specimen gauge length and in this way 'escape' from the high locking frequency. The AA 7020 alloy is much leaner in Mg-content (1.18 wt%), but has a high Zn-content. The diffusivity of Zn is believed to be higher than Mg at room temperature (see Table 2); this high Zn-content is fare from compensating the lower Mg-content when the band rate evolution is under concern. The reason for this is probably due to the much lower atomic size mismatch between zinc and aluminium (-7% difference) than between aluminium and magnesium (+11.9% difference) (see Table 3). The lower atomic size mismatch is believed to give much less interactions between solutes and dislocations for the case of Zn, hence, reducing the need to 'escape' from the presently deforming zone. This in-turn reduces to band rate as compared to the Mg-dominated case seen in alloy 5082. The DSA effect has also been observed in the alloy AA 2219 (A-type of serrations)

## ABSTRACT

### PLASTICITÀ DINAMICA IN SOLUZIONE SOLIDA. OSSERVAZIONI E QUANTIFICAZIONE

*Sono state effettuate rilevazioni su tre diverse leghe, AA 5082, AA 7020 ed AA 2219, per studiare il comportamento delle bande di deformazione dovute all'effetto di Portevin-Le Chatelier, che si determina nel corso della prova di trazione a temperatura ambiente. Durante la prova è stata applicata in situ una tecnica laser particolare, recentemente sviluppata e denominata Laser Speckle Technique (LST). Questa tecnica permette di conoscere le caratteristiche della banda di deformazione, in particolare relativamente alla velocità di banda $V_{band}$ e alla larghezza di banda $W_{band}$. I risultati ottenuti con il metodo LST si sono rivelati utili per capire i meccanismi alla base del limite di formabilità in presenza di sensibilità negativa della velocità di deformazione. Dalle indagini sono state tratte le seguenti conclusioni:*

- *Tutte le leghe studiate, allo stato solubilizzato, hanno mostrato un chiaro fenomeno DSA-PLC alle velocità di deformazione tra $1x10^{-3}$ e $1x10^{-4}$ $s^{-1}$, osservabile anche a $1x10^{-1}s^{-1}$.*
- *Le caratteristiche della banda sono controllate dalla interazione tra gli atomi e non dalla morfologia del grano, come ad esempio il fenomeno di DSA.*
- *Il limite di formabilità viene raggiunto quando la velocità PLC della banda raggiunge il suo più basso regime e dà luogo alla formazione delle bande di taglio.*
- *L'esperienza in situ ottenuta con la tecnica laser LST si è rivelata molto utile per capire e caratterizzare la natura della propagazione del fenomeno PLC e il limite di formabilità del materiale.*